PIC simulations of the competition of collisional and collisionless processes in the relaxation of the eVDF in the young solar wind

J. Völp[1] (jurek.voelp@rub.de), K. Schoeffler[1], A. Tenerani[2], and M. E. Innocenti[1]

[1]Institut für Theoretische Physik 1, Ruhr University Bochum, 44801 Bochum, Germany

[2]Department of Physics, The University of Texas at Austin, TX 78712, USA

Abstract As the solar wind expands in the inner heliosphere, the evolution and relaxation of the electron velocity distribution function (eVDF) is governed by a complex interplay of collisional and collisionless processes. This study investigates with **fully kinetic numerical simulations** the **competition between Coulomb collisions** and **the electron firehose instability (EFI)** - a kinetic instability arising under anisotropic pressure conditions in magnetized plasmas - during the isotropization of the electron VDF. The goal is to gain deeper insights into how collisional and collisionless processes influence each other in this regime. Simulations are run using the **particle-in-cell (PIC) code OSIRIS**, in the presence and absence of Coulomb collisions. The plasma density is progressively increased (also beyond physically motivated values) to increase the collision frequency and investigate plasma regions with significantly different temperatures.

Electron Firehose Instability in the Solar Wind

Solar wind observations have shown that Coulomb collisions have an influence on the electron heat flux regulation [1]. As preliminary study we have investigated the electron firehose instability (see Figure 1: EFI observations in the solar wind) and its competition with collisions. In this study, the non-resonant EFI branch is investigated with 1D PIC simulations (OSIRIS [3]) and validated against linear dispersion relations obtained with the code ALPS [4].

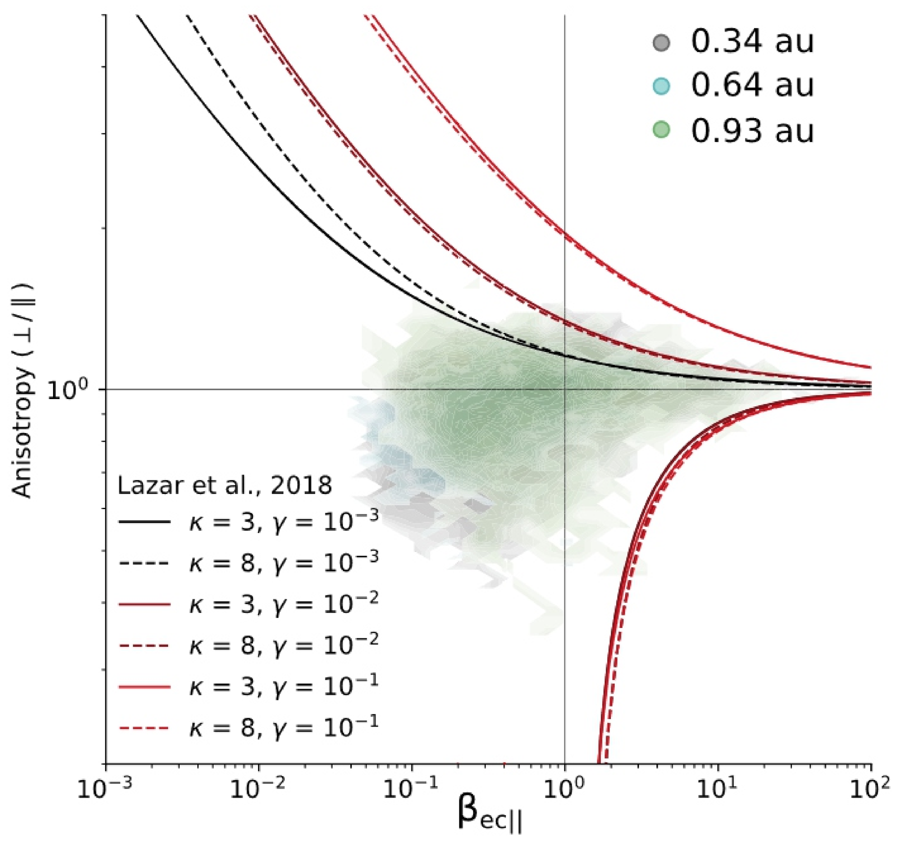

Fig. 1 Radial evolution of the solar wind core electrons. The anisotropy A is the ratio between the perpendicular and parallel temperature. β_e is the parallel plasma beta of the core electrons. The curves show the marginal stability thresholds for the whistler instability ($A > 1$) and the firehose instability ($A < 1$). The image is taken from Berčič et al. [2].

References

[1] S.D. Bale et al. (2013), *The Astrophysical Journal 769 L22*

[2] L. Berčič et al. (2019), *MNRAS 486.3*

[3] R. A. Fonseca et al. (2002), *Computational Science—ICCS 2002*

[4] D. Verscharen et al. (2018), *Journal of Plasma Physics 84.4*

Methods

To study the interplay between the EFI and Coulomb collisions, we systematically varied the plasma density. Given classical thermal velocities and Alfvén speeds, we can convert from simulation parameters using the following scaling relationship:

$$T_{\text{real}} = \left(\frac{n_{\text{real}}}{n_{\text{sim}}}\right)^{1/4} T_{\text{sim}}$$

where T_{sim} and n_{sim} is the simulation temperature and density, T_{real} and n_{real} are the real plasma temperature and density, respectively. Table 1 shows the simulation densities we used and the corresponding thermal energies of the electrons.

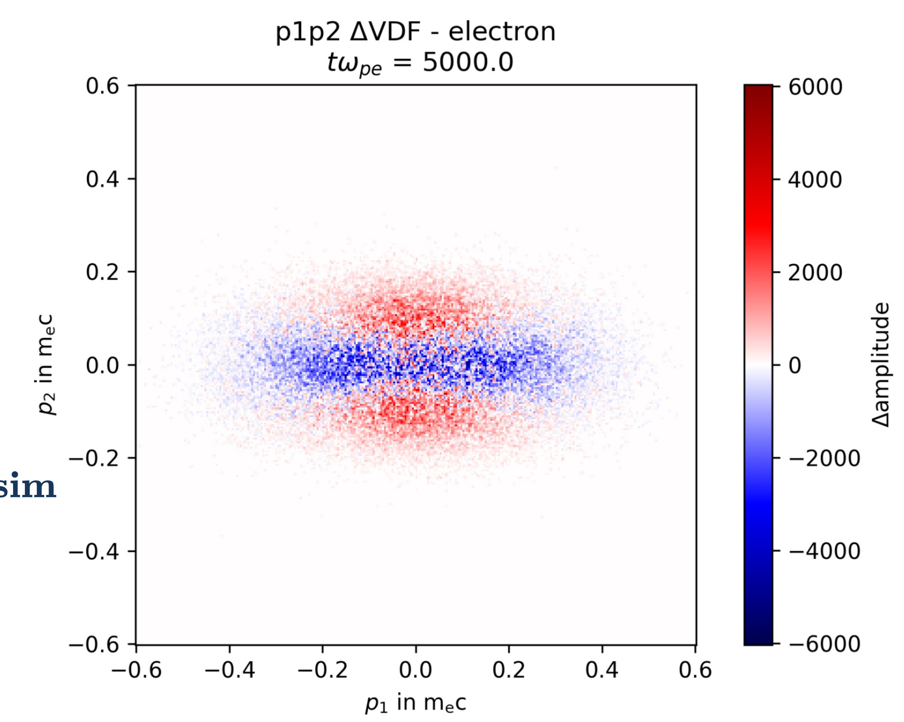

Fig. 2 Difference between the VDF of an EFI simulation without and with collisions during the linear phase of the instability with initial values of β_e=5 and A = 0.1.

Results

For every density, the initial temperature anisotropy is varied between $A = 0.1 - 0.5$ for a parallel plasma beta of β_e=5. Figure 2 shows the difference between the VDF of an EFI simulation w/o and w/ collisions during the linear phase. Figure 3 shows the evolution of the parallel plasma beta and the anisotropy as a function of time. Figure 4 shows that the growth rate of the instability remains relatively constant up to a simulated density of 10^{20} cm^{-3}, after which a cut-off is observed, which also depends on the initial anisotropy. The transition to a collisional regime occurs at temperatures close to 0.1 eV, which is too low for the solar wind.

Table 1 Simulation densities and the corresponding electron thermal energies

$n_{\text{sim}}/\text{cm}^{-3}$	$E_{th,\text{real}}/\text{eV}$
1.00×10^{12}	1.29×10^{1}
1.00×10^{16}	1.29×10^{0}
1.00×10^{20}	1.29×10^{-1}
1.00×10^{21}	7.27×10^{-2}
1.00×10^{22}	4.09×10^{-2}
1.00×10^{23}	2.30×10^{-2}
1.00×10^{24}	1.29×10^{-2}

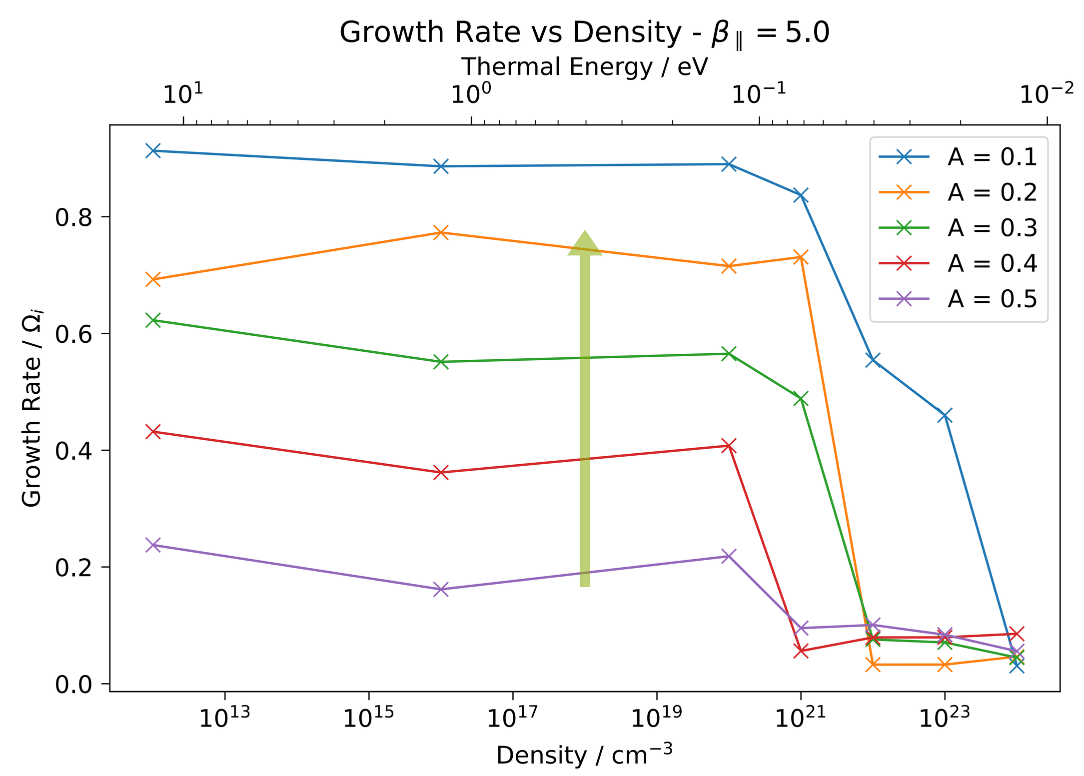

Fig. 4 Growth rates from OSIRIS simulations as a function of the collision density and the initial temperature anisotropy A for $\beta_{\parallel}$ = 5. The arrow points in the direction of increasing anisotropy.

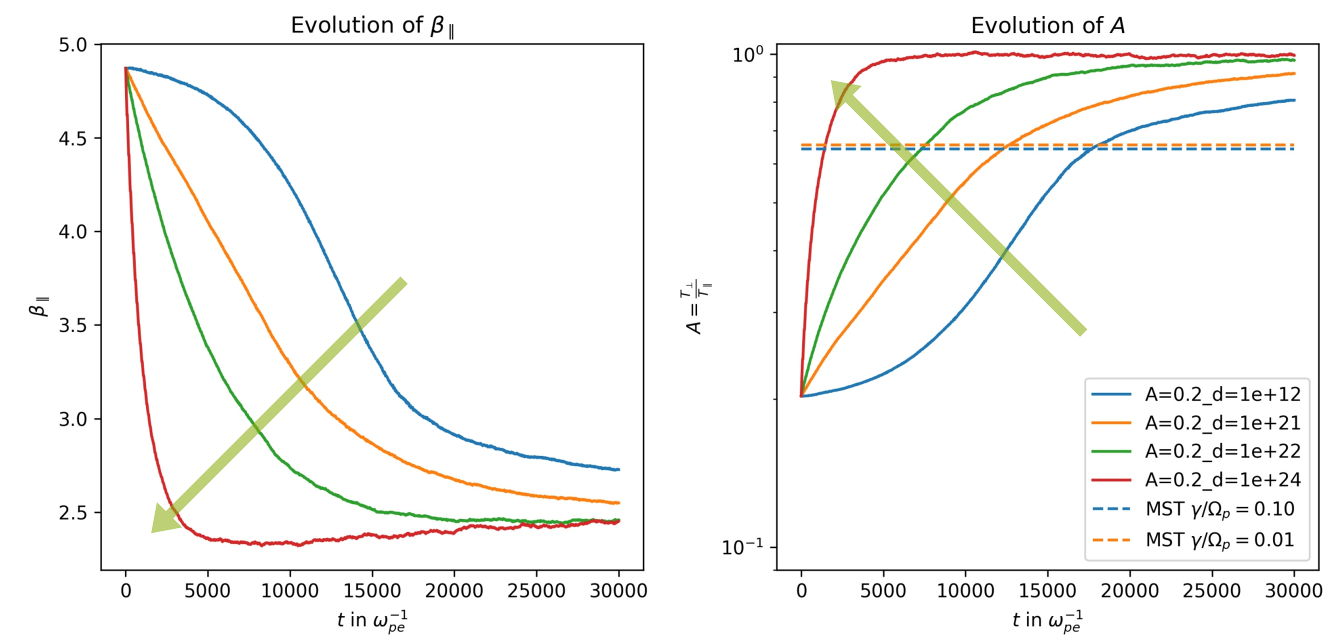

Fig. 3 Time evolution of $\beta_{\parallel}$ and A for initial values of A = 0.2 and $\beta_{\parallel}$ = 5. The dashed lines are the marginal stability thresholds for the initial $\beta_{\parallel}$. The arrows point in the direction of increasing collisionality.

Outlook

This work has to be intended as a preliminary study on competition of collisional and collisionless processes in the solar wind. While competition between EFI and Coulomb collisions is highly unlikely, future work will investigate different instabilities (e.g., the whistler heat flux instability) and competition in expanding plasmas.